

Metal hardening in atomistic detail

Luis A. Zepeda-Ruiz¹, Alexander Stukowski², Tomas Oppelstrup¹, Nicolas Bertin¹, Nathan R. Barton¹, Rodrigo Freitas^{3,4}, Vasily V. Bulatov^{1*}

¹Lawrence Livermore National Laboratory

²Technische Universität Darmstadt

³University of California Berkeley

⁴Stanford University

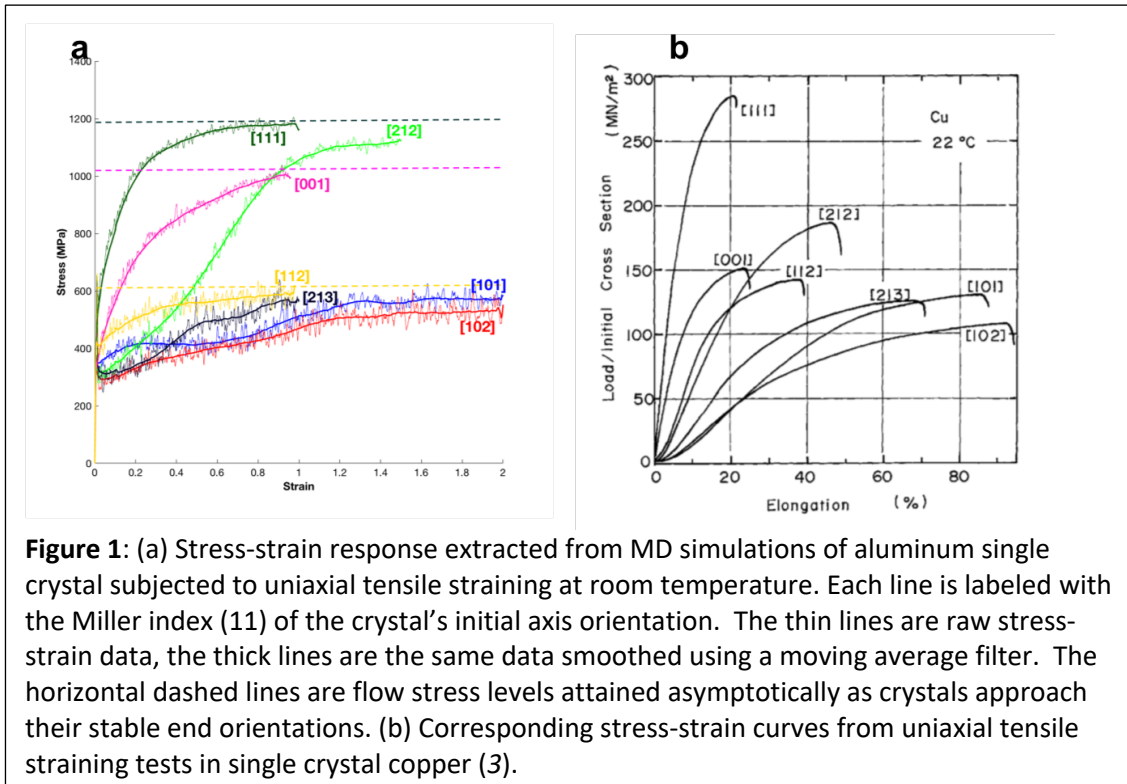
*Correspondence to: bulatov1@llnl.gov

Through millennia humans knew about and exploited the marvelous natural property of metals to harden under mechanical loads - a material is said to harden if it grows stronger when mechanically strained or deformed. Root causes of metal hardening remained unknown until 85 years ago when dislocations – curvilinear crystal defects made of lattice disorder - were proposed to be responsible for crystal plasticity. Yet, even though direct causal connection between dislocations and crystal plasticity is now firmly established, no quantitative theory exists to predict metal hardening directly from the underlying behavior of lattice dislocations. This has not been for lack of trying as numerous theories and models sprang to life explaining, often based on differing if not opposing viewpoints, metal hardening from dislocation mechanisms (1). But as physicist Alan Cottrell opined, work (strain) hardening is perhaps the most difficult remaining problem in classical physics (worse than turbulence) and is likely to be solved last (2). The essential difficulty in putting to rest still ongoing debates on mechanisms of strain hardening has been our persistent inability to observe what dislocations do *in situ* – during straining – in the material bulk.

While physicists grapple to understand and quantify strain hardening, material models employed to optimize metal processing (e.g. forging, rolling or extrusion) remain phenomenological and based on empirical observations largely predating the very concept of crystal dislocations. Here we rely on a super-computer to clarify what causes metal hardening. Instead of trying to derive hardening from the underlying mechanisms of dislocation behavior – which has been the aspiration of dislocation theory for decades - we perform ultra-scale computer simulations at a still more basic level: the motion of atoms the crystal is made of. Viewed here as unbiased computational experiments, in our simulations we observe, rather than prescribe, exactly how the motion of individual atoms translates into the motion of dislocations that then conspire to produce metal hardening. Here we focus our attention on clarifying the origins of so-called “three-stage” hardening as perhaps most argued-about aspect of metal plasticity.

Fig. 1a shows stress-strain response observed in our molecular dynamics (MD) simulations of seven aluminum single crystals subjected to uniaxial tension at ambient temperature and pressure. Shown in Fig. 1b are results of uniaxial tension experiments

on the same seven crystals reported by Takeuchi in his classic 1975 paper (3). Leaving aside for now quantitative differences in the magnitude of the flow stress, the simulated and experimental stress-strain curves are in remarkable qualitative agreement. Indeed, relative ordering of the flow stress among seven simulated crystals is the same as in the Takeuchi's experiment both in the early as well as in the late stages of straining. Still more striking is the agreement in the shapes of the seven response curves: whereas three crystals labeled [001], [111] and [112] exhibit simple "parabolic" stress rise (hardening), the other four curves show more or less distinct inflection, or "three-stage" hardening. The difference among the seven crystals was in the orientations of their crystal lattices (with respect to the straining axis), selected here after Takeuchi so as to sample important lattice orientations of a cubic crystal. Essential for this work is that in his paper Takeuchi also reports if and how each of the seven crystals rotates in response to tensile straining (3). Even though Takeuchi's results are for copper, qualitatively similar response has been widely reported in aluminum studied here and in most other face-centered cubic (FCC) metals (4-10).



The striking similarities between the two sets of stress-strain curves shown in Figs. 1a and 1b cannot be accidental despite an astonishing 10 orders of magnitude difference in straining rates: $5 \cdot 10^7/s$ in our simulations and $3 \cdot 10^{-3}/s$ in the experiment (3). This agreement suggests that: (a) fundamental physical mechanisms of dislocation plasticity remain invariant across the entire range of straining rates from low or "quasi-static" rates of experiments ($10^{-5} - 10^1/s$) to high or "dynamic" rates of our simulations ($10^5 - 10^8/s$); (b) viewed as computational experiments, our high-rate MD simulations are just

as quasi-static as the real low-rate laboratory experiments. Seemingly contradictory, the latter proposition derives from the following insights.

Often applied to straining experiments at rates exceeding $10^1/s$, the moniker “dynamic”, essentially means that straining conditions – straining rate, temperature, pressure, etc. – cannot be maintained stationary at such rates in a real laboratory test primarily due to a finite rate of heat exchange and to inevitably imperfect control over straining apparatuses. This is in contrast to low-rate “quasi-static” experiments in which straining conditions can and usually are maintained strictly stationary. Yet, despite very high rates of straining necessitated here by the notorious time limit of MD simulations, our “computational experiments” are essentially quasi-static as we employ special controls – “Maxwell’s demons” of sorts – that react to and gently nudge the motion of individual atoms so as to maintain the overall temperature, pressure and straining rate stationary. While the total duration of our simulated MD trajectories is in the range 20-40 ns, this is still far longer than characteristic time scales of dislocation motion that delineate truly dynamic from quasi-static response. For instance, it takes only a few ps for a dislocation to adjust its velocity to a change in local stress (dislocation inertia), or a fraction of one ns for the same dislocation to travel from one obstacle to another. Thus, even if flow stress, dislocation density and other rate-dependent measures of metal plasticity reported here are understandably different, we sustain that, with respect to the underlying dynamics of dislocation behavior, our high-rate MD simulations are just as quasi-static as the low-rate laboratory experiments. Thus our observations presented below should be representative of quasi-static metal plasticity across the entire range of accessible straining rates.

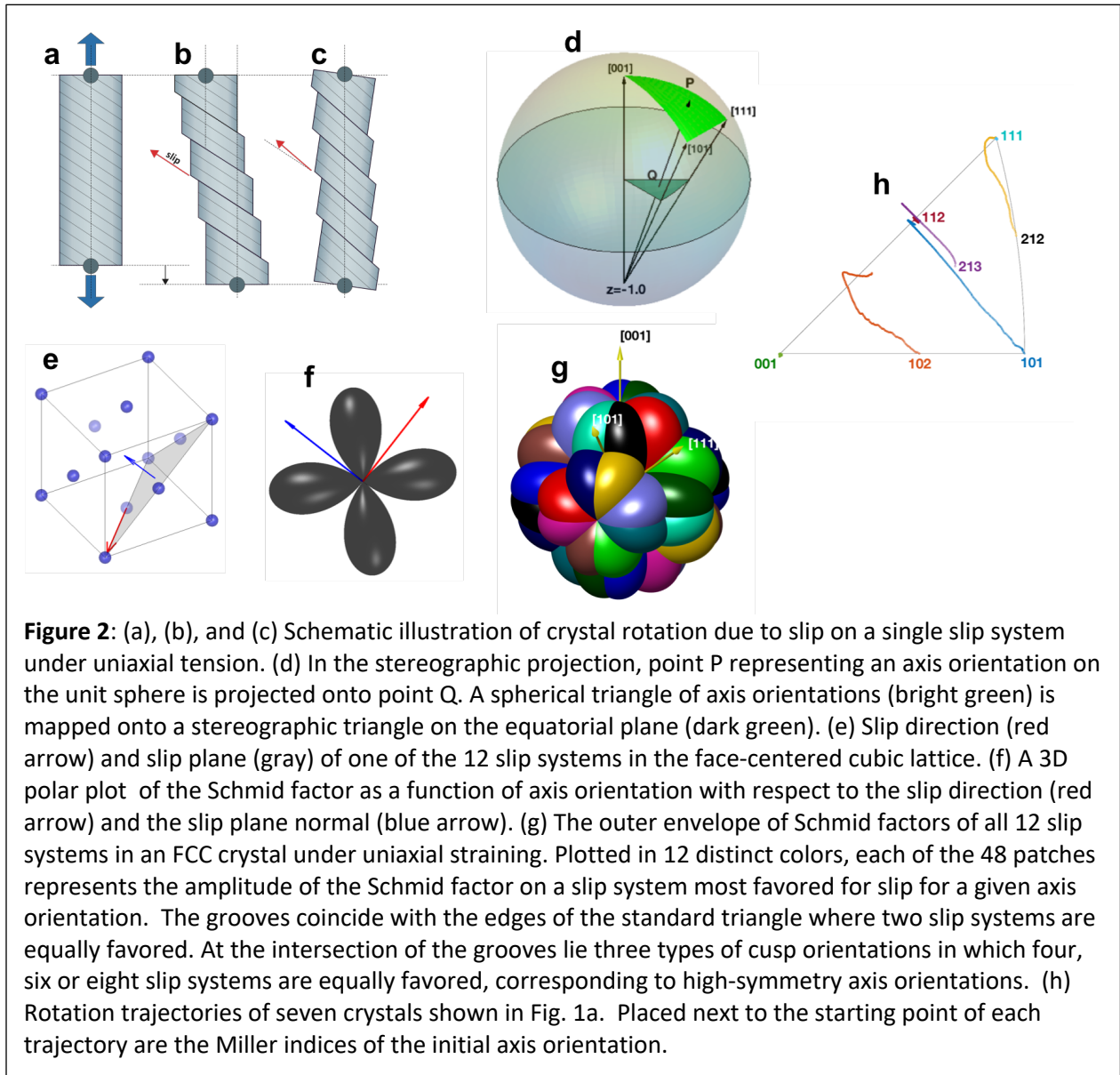
Our key observation is that staged hardening is a direct manifestation of crystal rotation. Listed in Table 1 in order of decreasing initial slip symmetry, characteristic variations in the shapes of stress-strain curves are directly attributable to the occurrence (or not) of crystal rotation during straining. Three-stage (inflection) hardening is observed in the five crystals that we observe to rotate under straining whereas parabolic hardening without an inflection is observed in the curves of the three crystals that do not rotate.

Table 1: Qualitative characteristics of strain hardening observed in MD simulations.

Initial axis	Initial slip symmetry	Crystal rotates?	Hardening response	End axis
[001]	8-fold, holds*	no	parabolic	[001]
[111]	6-fold, holds	no	parabolic	[111]
[101]	4-fold, breaks*	yes	3-stage	[112]
[112]	2-fold, holds	no	parabolic	[112]
[212]	2-fold, holds	yes	3-stage	[111]
[102]	2-fold (breaks	yes	3-stage	[112]
[213]	no symmetry	yes	3-stage	[112]
[8,5,13]**	no symmetry	yes	3-stage	[112]

* “Breaks” and “holds” indicate, respectively, whether or not the initial crystal orientation experiences symmetry-breaking under straining.

**Not shown in Fig.1a, stress-strain response of this crystal orientation is very similar to the [213] case.

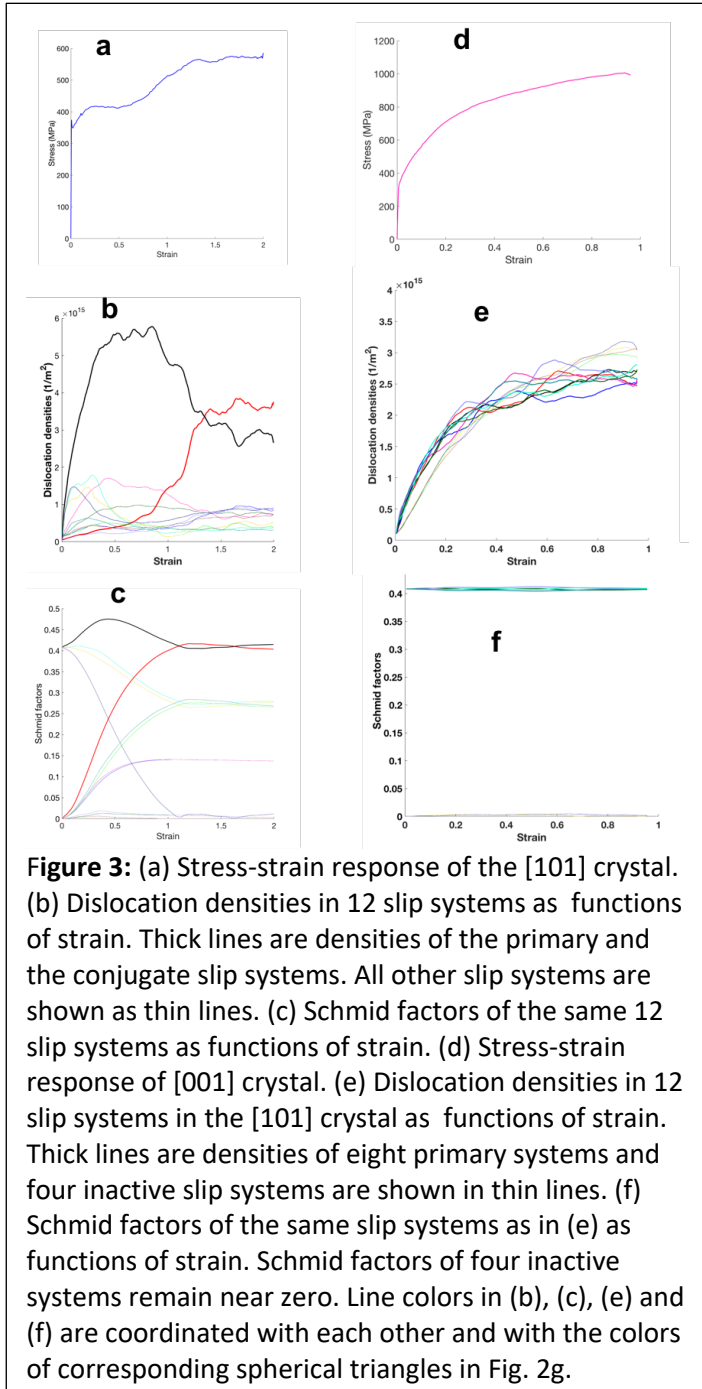


It turns out to be possible to explain why and, to a lesser extent, how crystals rotate under uniaxial straining without ever invoking lattice dislocations. About a century ago, well before lattice dislocations were first hypothesized (12-14) and later observed (15), it was discovered that single crystals, i.e. crystals with the same lattice orientation across the entire specimen volume, respond to straining by slipping in specific lattice planes along specific lattice directions (16-18), Fig. 2a: each such pair of a slip plane and a slip direction constitutes a slip system. In most crystals several such slip systems exist that can potentially contribute to macroscopic slip. Based on empirical observations, the

celebrated Schmid law states that, when multiple slip systems exist, slip occurs in systems that are most favorably inclined with respect to the straining axis: this preference for slip is commonly expressed by the geometric Schmid factor (19). Schmid also rationalized why some single crystal specimens rotate under uniaxial straining (20). As shown in Fig. 2b, when orientation of the straining axis is such that one of the crystal's systems is most favorably inclined for slip, slipping along this primary slip vector should skew the specimen's shape. However the specimen is constrained to stay co-axial with the grips of a stiff straining machine and compensates for its inability to skew by rotation, Fig. 2c. Based on such purely geometrical considerations, Schmid predicted that under tension a crystal should rotate so as to align its dominant slip direction with the straining axis (21). Conversely, in a frame tied to the crystal lattice the straining axis rotates towards the dominant slip direction.

Takeuchi (3) selected his seven crystal orientations so as to sample all possible symmetries with respect to the straining axis of the face-centered cubic (FCC) lattice. To follow the logic it is convenient to use the stereographic projection (Fig. 2d) and to map orientations of the straining axis onto the so-called standard triangle that constitutes just 1/48 of the unit sphere of axis orientations. Owing to the high symmetry of the cubic lattice, axis orientations within just one such triangle represent all other possible axis orientations. The standard triangle is particularly convenient for understanding slip crystallography in FCC crystals, because for every axis orientation in the interior of each triangle exactly one of the 12 slip systems – the primary system - is most favorably inclined for slip under uniaxial extension (Figs. 2e, 2f, 2g). Axis orientations on triangle edges are shared by two adjacent triangles and have at least two equally favored slip systems seeing the highest Schmid factor. Triangle corners [101], [111] and [001] lie at the intersections of two, three and four triangle edges and straining along these corner axes equally favors slip in four, six and eight slip systems, respectively. In SM we augment Schmid's geometric arguments with an *a priori* slip stability and reorientation flow analyses to predict which of the crystals studied here should rotate and which should not and, for each crystal predicted to rotate, where it should rotate to.

All but one crystal orientation behave precisely as predicted (Fig. 2h). Three crystals with axis orientations [001], [111] and [112] do not rotate at all. Crystals [213], [102] and [101] all eventually rotate to [112]. However, unlike crystal [213] that has no slip symmetry to begin with, crystals [102] and [101] break their initial 2-fold and 4-fold slip symmetries before they begin to rotate. Also predicted to break its 2-fold slip symmetry and then rotate to [112], crystal [212] instead retains its symmetry and rotates towards [111] along the [101]-[111] triangle edge. Even though we are yet to understand why this crystal rotates not as predicted, its rotation trajectory too agrees with Takeuchi's and other experiments (5). This lends additional support to our observation that, despite their vastly different straining rates, our simulations and laboratory experiments probe the same physics of crystal plasticity. Since MD simulations allow unfettered



The simulated straining response of an aluminum crystal initially oriented along the [101] axis is shown in Fig. 3a. Although all 12 slip systems were initially equally populated with dislocations, the density of dislocations in the preferred four slip systems grows quickly from the start reflecting high slip activity in them, as shown in Fig. 3b. Owing to mutual forest resistance of intersecting dislocations in the four active systems the initial post-yield rate of hardening is high - when observed, such initially rapid hardening is sometimes referred to as stage-0 hardening. Soon the initial 4-fold symmetry breaks and one of the four systems (black line) continues to multiply

access to every detail of atomic motion *in situ*, it should be possible to eventually establish what causes this and other still unexplained behaviors in metal plasticity.

To understand *why* and *how* crystal rotation causes staged hardening here we take advantage of our unique ability to see what dislocations do *in silico*, during straining in an MD simulation. Unlike mesoscale method of Discrete Dislocation Dynamics (DDD) that prescribes how dislocations respond to mechanical stress caused by straining (22,23), our approach is much more basic – we only specify how aluminum atoms interact with each other (24). We then extract dislocations from atomistic configurations encountered every 0.1 ns along the simulated straining trajectories and partition the so-extracted dislocations over 12 slip systems of the FCC crystal. Fig. 3 presents two out of seven straining simulations in which stress response, slip activity and Schmid factors of all 12 slip systems are coordinated along the straining trajectories.

dislocations while dislocation densities in three other initially favored systems (green, yellow and blue) subside. This causes the forest resistance and the hardening rate to drop entering what is called easy glide or stage I hardening. Just as predicted by Schmid, when one slip system dominates, the straining axis rotates towards its primary slip direction [011]. While the axis rotates across the triangle (Fig. 2h), the primary system becomes still more favored (note the maximum in its Schmid factor in Fig. 3c) so that the flow stress stays flat or even decreases slightly. On approaching the triangle edge, another “conjugate” system begins to see increasing Schmid factor (dashed red line in Fig. 3c) and gradually activates. Dislocations in the conjugate system become more numerous increasingly blocking the motion of primary dislocations and causing the flow stress to rise more rapidly again due to increasing mutual forest resistance between the two active systems – this is hardening stage II. Schmid factors on the conjugate and primary systems become equal precisely when the axis crosses the triangle edge, but the axis trajectory slightly overshoots the edge and only then returns to it and settles at [112]. Observed in experiments, axis overshoot and subsequent axis oscillations are manifestations of “latent hardening” caused by delayed dislocation multiplication first in the conjugate system, then in the primary system, etc. As the axis settles in its end [112] orientation, both the flow stress and the fractional dislocation densities gradually approach their asymptotic values, with the associated reduction in hardening rate marking the transition to stage III. As was argued before (1) and supported by our recent results (25), asymptotic saturation of the flow stress and dislocation density can be achieved when dislocation multiplication is exactly balanced by dislocation annihilation. In real experiments such asymptotic saturation is invariably interrupted by a macroscopic catastrophe such as necking and fracture or barreling so that the impending flow stress saturation is hinted at but not fully resolved in the experimental stress-strain curves (Fig. 1b) (3). Although previously reported in the literature, most of these dislocation activity and evolution behaviors in staged hardening were inferred from circumstantial evidence, such as surface slip trace analysis and *postmortem* electron microscopy. Having access to all of the details of simulated atomistic trajectories, we produced several videos illustrating how much more insight can be gained by observing what dislocations do *in silico* in material bulk.

Staged hardening observed in MD simulations of other crystal orientations is just as tightly connected to crystal rotation however detailed evolution of slip systems observed in MD simulations varies from case to case. Three tested crystals with orientations [001], [111] and [112] do not rotate, retain their initial symmetries and show no staged hardening (Fig. 1a). Considering [001] straining as a representative example (Fig. 3d), evolution of dislocation populations in 12 slip systems observed in these three simulations is rather uneventful: all initially favored systems remain equally favored (Fig. 3e) and active through straining as is evidenced by a steady rise and eventual saturation of dislocation densities in all active slip systems. A surprising result however is that dislocations in systems with zero Schmid factors multiply nearly as much or even more than the active systems. In particular, under [001] straining, asymptotic density produced in each of the four “inactive” systems exceeds asymptotic densities in

each of the eight active systems (Fig. 3e). First reported in (26), generation of dislocations in nominally inactive systems via junction reactions is a potentially important contribution to latent hardening broadly defined as any effect of active systems on the behavior of inactive systems (27). We expect such latent multiplication of “dislocation dark matter” to be consequential for metal plasticity.

In addition to eight simulations reported in table 1 (seven of which are shown in Fig. 1a), we performed smaller (~ 40 million atoms) simulations of six additional initial axis orientations. Out of 14 crystal orientations, all but three crystals are observed to be unstable and, when strained to a sufficiently large strain, asymptotically rotate towards one of the three stable “attractor” orientations. Thus, all possible crystal orientations naturally partition themselves into non-overlapping conical patches in orientation space, each cone centered on one of the three attractor orientations. On approaching their respective end orientations, rotating crystals raise their symmetry to double-slip (all the ones rotating to [112]), to sextuple-slip (approaching [111]) or to octuple-slip (approaching [001]). Flow stress attained in each of the three asymptotic attractor orientations is maximum over all orientations from the same conical patch (three dashed lines in Fig. 1a): within their local cones of attraction the three stable orientations are both the strongest and most symmetric. Our analysis of axis stability (see SM) further predicts that the [001] orientation should be only marginally stable under tension. Fittingly, we are yet to find a single initial axis orientation to rotate towards [001]: the cone of orientations attracted to [001] appears to be narrow. The ability to simulate lattice reorientation at very large strains and to identify asymptotic attractor orientations in MD simulations is important for improving accuracy of engineering models used to predict evolution of polycrystalline texture in rolling, forging, extrusion, ECAP, and other metal-forming operations.

Evidence is abundant in the literature that staged hardening in single crystals is a general phenomenon not limited to aluminum, FCC metals or cubic crystals and is observed in metals, semiconductors and ionic crystals alike. Our simulations clarify that three-stage hardening is not an intrinsic material property, but a kinematic consequence of the co-axiality constraint imposed on specimens in the standard uniaxial tests. Thus, it makes little sense to seek explanations of staged hardening in dislocation mechanisms somehow changing from one hardening stage to the next. At the same time, our simulations bring to light several previously unknown and potentially important aspects of metal plasticity that require one to delve more deeply into the details of dislocation motion for an explanation. Having access to the entire MD trajectory and armed with our recently developed methods of *in silico* computational microscopy (28,29), we can now relate every wiggle in the stress-strain response to underlying events in the life of atoms and dislocations. If, as we posit, our high-rate MD simulations and low-rate experiments probe the same physics, simulations of the kind presented here offer unique means for inquiry into fundamentals of crystal plasticity.

REFERENCES AND NOTES

1. U. F. Kocks, H. Mecking, Physics and phenomenology of strain hardening: the FCC case. *Progress in Materials Science* **48**, 171-273 (2003).
2. A. H. Cottrell, Commentary. A brief view on work hardening. In: *Dislocations in Solids* **11**, vii-xvii (2002).
3. T. Takeuchi, Work hardening of copper single crystals with multiple glide orientations. *Trans. JIM* **16**, 629-640 (1975).
4. K. Lücke, H. Lange, Über die Form der Verfestigungskurve von Reinstaluminiumkristallen und die Bildung von Deformationsbandern. *Zeitschrift für Metallkunde* **43**, 55-66 (1952).
5. W. Staubwasser, Über die Verfestigung von Aluminium Einkristallen (99.99% Al) und ihre Deutung, *Acta Metall.* **7**, 43-50 (1969).
6. L. M. Clarebrough, M. E. Hargreaves, The orientation dependence of work-hardening in crystals of face-centered cubic metals, *Australian Journal of Physics* **13**, 316-325 (1960).
7. F. R. N. Nabarro, Z.S. Basinski, D.B. Holt, The plasticity of pure single crystals. *Advances in Physics* **13**, 193-323 (1964).
8. T. S. Noggle, J. S. Koehler, Electron microscopy of aluminum crystals deformed at various temperatures. *J. App. Phys.* **28**, 53-62 (1957).
9. J. Garstone, R. W. K. Honeycombe, G. Greetham, Easy glide of cubic metal crystals. *Acta Metall.* **4**, 485-494 (1956).
10. W. F. Hosford, R. L. Fleischer, W. A. Backofen, Tensile deformation of aluminum single crystals at low temperatures. *Acta Metall.* **8**, 187-199 (1960).
11. W. H. Miller, A treatise on crystallography. (1839) 139 pp.
12. E. Orowan, Zur Kristallplastizität. *Z. Phys.* **89**, 605-659 (1934).
13. G. Taylor, The mechanism of plastic deformation in crystal. Part I. Theoretical. *Proc. R. Soc. A* **145**, 363-404 (1934).
14. M. Polanyi, Über eine Art Gitterstörung, die einen Kristall plastisch machen könnte. *Z. Phys.* **89**, 660-664 (1934).
15. P. B. Hirsch, R. W. Horne, M. J. Whelan, Direct observations of the arrangement and motion of dislocations in aluminium. *Philos. Mag.* **86**, 677-684 (1956).
16. W. Rosenhain, Further observations on slip-bands in metallic fractures. Preliminary note. *Proc. Roy. Soc. London* **74**, 557-562 (1905).
17. J. Frenkel, Zur Theorie der Elastizitätsgrenze und der Festigkeit kristallinischer Körper, *Z. Phys.* **37**, 572-609 (1926).
18. E. Schmid, W. Boas, Kristallplastizität (vol. 17 *Struktur und Eigenschaften der Materie*, Verlag Julius Springer, Berlin 1935), 373 pp.
19. E. Schmid, Beiträge zur *Physik und Metallographie* des Magnesiums. *Zeitschrift für Elektrochemie und angewandte physikalische Chemie* **37** (447-459 (1931).
20. H. Mark, M. Polanyi, E. Schmid, Vorgänge bei der Dehnung von Zinkkristallen. *Z. Phys.* **12**, 78-110 (1923).
21. W. F. Hosford, Mechanical behavior of materials (Cambridge University Press, 2 edition, 2009), pp. 129-131.

22. L. P. Kubin, G. Canova, The modeling of dislocation patterns. *Scripta Metall.* **27**, 957-962 (1991).
23. V. V. Bulatov, W. Cai, Computer Simulations of Dislocations, 196–240 (Oxford Univ. Press, 2006).
24. X.-Y. Liu, F. Ercolessi, J.B. Adams, Aluminium interatomic potential from density functional theory calculations with improved stacking fault energy. *Modelling and Simulation in Materials Science and Engineering* **12**, 665-670 (2004).
25. L. A. Zepeda-Ruiz, A. Stukowski, T. Opperstrup, V. V. Bulatov, Probing the limits of metal plasticity with molecular dynamics simulations. *Nature* **550**, 492-495 (2017).
26. S. Aubry, M. Rhee, G. Hommes, V. V. Bulatov, A. Arsenlis, Dislocation dynamics in hexagonal close-packed crystals. *Journal of the Mechanics and Physics of Solids* **94**, 105-126 (2016).
27. M. Stricker, D. Weygand, Dislocation multiplication mechanisms – Glissile junctions and their role on the plastic deformation at the microscale. *Acta Mater.* **99**, 130-139 (2015).
28. A. Stukowski, Visualization and analysis of atomistic simulation data with OVITO — the Open Visualization Tool. *Model. Simul. Mater. Sci. Eng.* **18**, 015012 (2010).
29. A. Stukowski, K. Albe, Extracting dislocations and non-dislocation crystal defects from atomistic simulation data. *Model. Simul. Mater. Sci. Eng.* **18**, 085001 (2010).